A major impact of WRF planetary boundary layer schemes on simulation accuracy of vertical wind structure by 3D Doppler Wind Lidar

Lei Zhang [1,2,3] ·Jinyuan Xin [*1,2] ·Yan Yin [1] ·Wenyuan Chang [2] ·Min Xue [4] ·Danjie Jia[2] · Yongjing Ma[2]

Abstract

The accuracy of wind field simulation and prediction is one of the most significant parameters in the field of atmospheric science and wind energy. Limited by the observation data, there are few researches on wind energy development. A 3D Doppler wind lidar (DWL) providing the high-vertical-resolution wind data over the urban complex underlying surface in February 2018 was employed to evaluated the accuracy of vertical wind field simulation systematically for the first time. 11 PBL schemes of the Weather Research and Forecasting Model (WRF) were employed in simulation. The model results were evaluated in groups separated by weather (sunny days, haze days and windy days), observation height layers, and various observation wind speeds. The test results presented that the vertical layer altitude of the observation point position was the most important factor. The simulation is fairly well at a height of 1000-2000m, as most of the relative mean bias of wind speed and wind direction are less than 20% and 6% respectively. Below 1000 m, the wind speed and direction biases are about 30%-150% $m.s^{-1}$ and 6%-30% respectively. Moreover, when the observed wind speed was lower than 5 $m.s^{-1}$, the bias were usually large, and the wind speed relative mean bias is up to 50-300%. In addition, the accuracy of simulated wind profile is better in 10-15$m.s^{-1}$ than other speed ranges, and is better up 1000m than below 1000m in the boundary layer. We see that the WRF boundary layer schemes have different applicability to different weather conditions. The WRF boundary layer schemes have significant differences in wind field simulation with larger error under the complex topography. A PBL scheme is not likely to maintain its advantages in the long term under different conditions including altitude and weather conditions.

Keywords: 3D Doppler Wind Lidar; planetary boundary layer; vertical wind; wind speed; wind direction

1 Introduction

Wind Energy is an inexhaustible source of clean energy. The development of wind power plays an important role in improving energy structure, protecting ecological environment, ensuring energy security and achieving sustainable economic development. The utilization of wind energy attracts more and more international attention, but it still develops slowly, which is directly related to the instability and intermittence of wind speed. The prediction of boundary layer wind in a very worthy of study in the utilization of wind energy. The planetary boundary layer (PBL) is close to the tropospheric underlying surface, which strongly interacted with the atmosphere by turbulent exchanges of mass, energy and momentum in the PBL (Coantic et al. 1989). The PBL parameterizations affect the model performance largely on vertical eddy diffusivities, surface energy budget, tracer concentrations (e.g. water vapor) and the transport of air pollutants (Cheng et al. 2012; Han et al. 2009; Wei et al. 2017; Wang et al. 2012; Zhang et al. 2015). As the complexity of the thermodynamic processes associated with radiation, cloud physics, air dynamics, surface friction and anthropogenic sources for water vapor and heat, it is both critical and challenging to reproduce PBL wind structure and predict urban air quality (Zhan et al. 2017).

Many previous studies focused on comparing the observation data with boundary layer simulation were to discuss whether some kind of PBL schemes are suitable for a specific weather condition or type of terrain, in order to get an empirical conclusion to instruct numerical forecast.

The most commonly used observational data are ground observations. Cup anemometer data was used to compare with vertical wind speed and wind shear, it is predicated that different PBL schemes could be suitable for simulating wind fields under specific stable conditions (Hahmann et al. 2011). Wind speed above 10 m ground level were employed for the sensitivity of WRF model

* Corresponding author: Xin Jinyuan

Email: xjy@mail.iap.ac.cn

1 Collaborative Innovation Center on Forecast and Evaluation of Meteorological Disasters, Nanjing University of Information Science and Technology, Nanjing 210044, China,

2 State Key Laboratory of Atmospheric Boundary Layer Physics and Atmospheric Chemistry (LAPC), Institute of Atmospheric Physics, Chinese Academy of Sciences, Beijing 100029, China,

3 China Meteorological Administration Training Centre,

4 State Key Laboratory of Severe Weather/Institute of Atmospheric Composition, Chinese Academy of Meteorological Sciences (CAMS), CMA, Beijing 100081, China

with various initial conditions datasets to note that the nonlocal closure scheme such as YSU and ERA-Interim reanalysis data leads to the best estimation of wind speed (A Siavash et al. 2020).

Morever, there were some other observation data for verification. Upper air radiosonde was used to study the vertical structure characteristics and time evolution of the atmospheric boundary layer in an arid region of southwestern Algeria (Abdellali et al. 2011). ASAR-retrieved wind field was acquired for comparison with simulated wind structure (Miglietta et al. 2010). Data from 10 stations of the Japan Meteorological Agency's wind profiler network and data acquisition system (WINDAS) were employed to evaluate wind resources in coastal areas. The simulated annual average wind speed had a significant positive bias in the lower part of the PBL, which cannot be improved by alternative PBL schemes (Shimada et al. 2011). Micro pulse lidar estimates were evaluated against simulated PBL heights, which was proved to be underestimated, and also found that the nonlocal ACM2 scheme may be good choice (Banks et al. 2015, 2016). Turbulent flux measurements from FINO1 platform were used in different atmospheric stabilities analysis (Muñoz-Esparza et al. 2012).

In this study, we employed high-resolution 3D Doppler wind lidar (DWL) observations, which were rarely used in the previous studies, to evaluate the simulated atmospheric boundary layer wind fields with 11 PBL schemes under different weather conditions in Beijing. The objective of this study is to verify the importance of WRF planetary boundary layer parameterization schemes in wind simulation and the possible deviation by 3D Doppler Wind Lidar.

Section 2 describes the DWL data, the PBL schemes and the synoptic characteristics of our case. Section 3 analyzed the PBL wind speed profile, the horizontal and vertical wind speed and direction, and the Section 4 is the article conclusion.

2. Methodology and Data

2.1. The DWL Observation

The atmospheric turbulence leads to the fluctuation of refractive index, the movement of scattering layer and the movement of turbulence block. It can give rise to the turbulence scattering caused by the inhomogeneous refractive index of the atmosphere, and resulting in the Doppler frequency shift of the returned electromagnetic wave signal. The radial velocity relative to radar can be obtained by Doppler technology. Under certain assumptions, the wind direction, wind speed and vertical motion at the height of echo signal can be estimated by Doppler multi-direction velocity measurement.

The DWL in this paper was deployed in the research area of Institute of Atmospheric Physics, Chinese Academy of Sciences, located at the urbanization area between the north 3rd and 4th ring roads in Beijing. It can provide 24h uninterrupted measurements of meteorological elements such as the wind velocity, wind direction, temperature and atmospheric refractive index from 50 m to 3000 m above surface with a sampling resolution of 20 m per 20 seconds. Following the detection method of Brewster K A (1989), the accuracy of DWL data is verified by a 320 m observation tower, and the missing DWL data caused by strong noise in the near ground signal was eliminated.

2.2. Experimental design

WRF3.9 was used in this study. We conducted a set of model experiments, corresponding to 11 PBL schemes discussed in the context. Their abbreviations are YSU, MYJ, GFS, QNSE, MYNN2.5, MYNN3, ACM2, BouLac, UW, Shin-Hong, and GBM (Table 1). These schemes are either local or nonlocal closure.

The local closure estimates the unknown PBL quantities by the physical quantities or gradients, through predicting the turbulence perturbation kinetic energy (TKE) at the same place, while the nonlocal closure estimates quantities with many known physical quantities or gradients besides the unknown grid. The K-profile method of first-order closure is employed to address the turbulence closure schemes. YSU and ACM2 are nonlocal schemes, while the others are local schemes.

We set up three-nested domains centered at 116.68°E, 39.87°N (Figure 1). The horizontal resolutions were 27, 9 and 3 km, with the domain sizes of 100×94, 70×67 and 64×55 respectively. The outermost domain d01 covered most of China. The second domain d02 covered the North China Plain and the northwestern mountainous area including Beijing city. The third domain is the main research area, which near the Institute of Atmospheric Physics, Chinese Academy of Sciences. The atmosphere is divided into 43 layers vertically, including 29 layers below 2km, and the top layer is at 50 hPa. The physical parameterizations include the Dudhia shortwave radiation scheme, the Rapid Radiative Transfer Model longwave radiation scheme, the Kessler scheme for microphysical processes, and the Grell cumulus convection parameterization scheme. As is not suitable for this fine resolution, the cumulus convection scheme only applied in d01 and d02 regions, but turned off in d03. The model was driven by the NCEP/NCAR reanalysis data and integrated from February 24 to March 2, 2018, with additional 6 h for spin-up (Clark et al. 2007). The model results were output every half hour.

Figure 2 illustrates the observed DWL wind data in our case. The PBL wind was weak below 800 m height on February 24-25, indicating a stable boundary air. The PBL wind speed increased in the daytime on February 26, and the wind direction above 1000 m height changed from southwest to northwest. The wind slowed again on February 27 and became strong on February 28. At the middle troposphere, according to the MICAPS 4.0 analysis, a cold high pressure maintained at 500 hPa over northern China, and the low atmosphere was stable. On February 26, a shallow trough passed through Beijing, resulting on haze weather. From 14:00-17:00 UTC (Coordinated Universal Time) on February 28, a cold front induced an upper gale over Beijing and a gale at the ground at 17:00-20:00 UTC. After a short break with gentle winds, the southwest wind enhanced at 02:00 UTC on March 1.

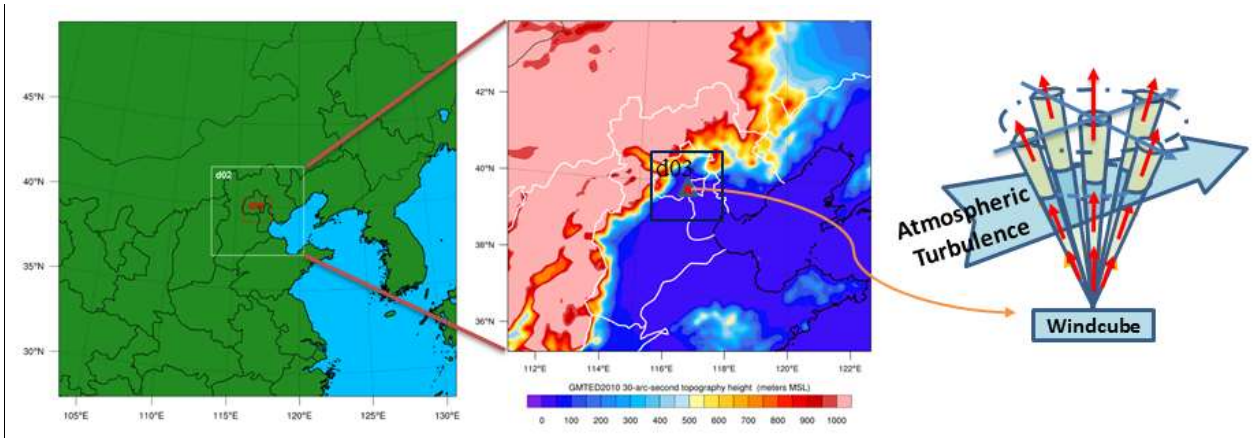

Fig. 1 The model topography (left, middle) and the schematic diagram of the DWL (right) deployed in the center of model domain (red point in the left).

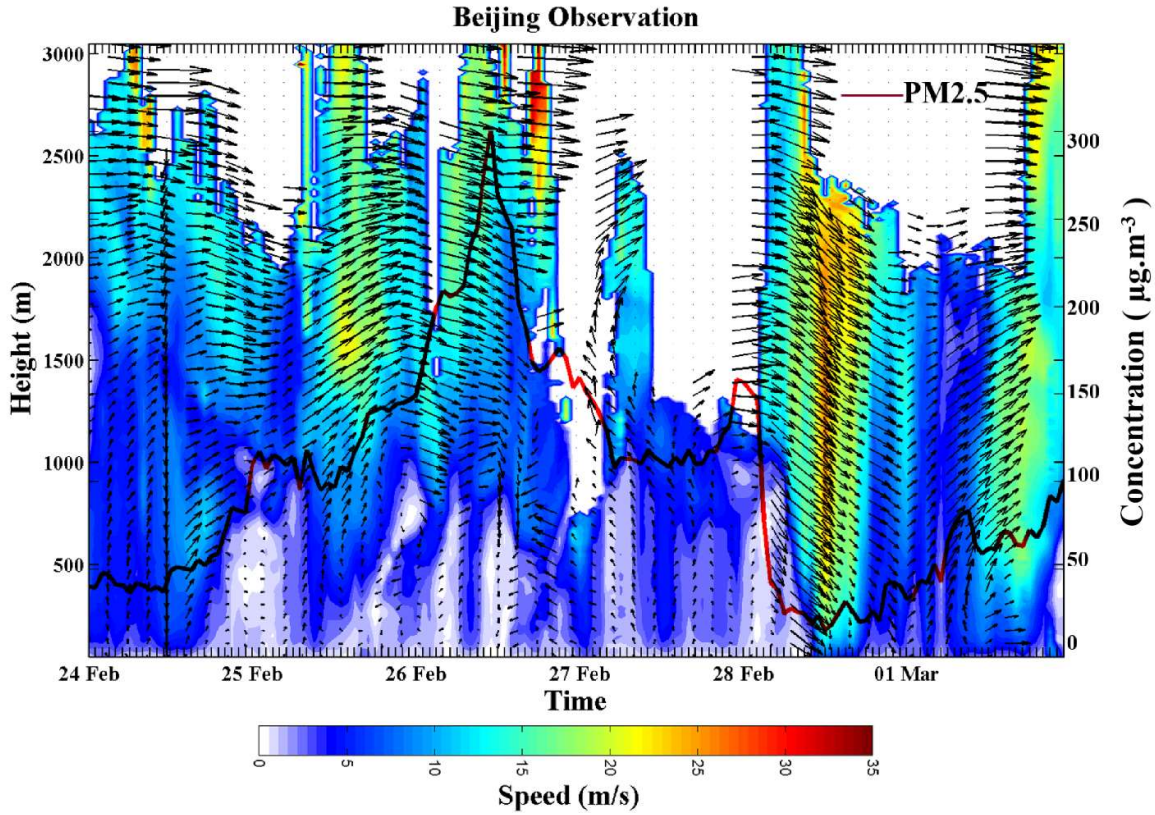

Fig. 2 The simulated $PM_{2.5}$ concentrations (red line) and the PBL wind structures in Beijing, February 2018

Table 1 Comparison of 11 planetary boundary layer schemes

Options	Schemes	Closure methods	Mixing processes for unstable boundary layers	Main features
1	Yonsei University (YSU)	Nonlocal	K-Profile Method, First Order Closed Model	Considers the influence of entrainment process at the top of mixed layer on turbulent transport; the height of PBL depends only on the buoyancy profile (Hong et al. 2006)
2	Mellor-Yamada-Janjic Scheme (MYJ)	Local	Turbulent kinetic energy (TKE) closure scheme, 1.5-order closure model	It was suitable for studying fine PBL structure. The height of PBL was determined by the turbulent energy profile (Janjic 1994)
3	NCEP Global Forecast System	Nonlocal	First-order vertical mixing scheme	The height of the PBL was determined by the iterative bulk Rechardson method from the surface up integration. The diffusion

	(GFS)			coefficient above surface was a cubic function of the height of the PBL, and its coefficient value was obtained by the coupled surface flux. (Hong et al. 1996)
4	Quasi-normal Scale Elimination (QNSE)	Local	TKE Closing Scheme, 1.5 Order Closing Model	The physical process was complex and suitable for the prediction and simulation of the PBL in the stable layer region (Sukoriansky et al. 2005)
5	Mellor-Yamada Nakanishi Niino (MYNN) Level 2.5	Local	TKE Closing Scheme, 1.5 Order Closing Model	Improvement of MYNN3 limits the ratio between the main length scale and TKE (Mikio and Hiroshi 2006)
6	Mellor-Yamada Nakanishi Niino (MYNN) Level 3	Local	TKE Closing Scheme, 2 Order Closing Model	Considered the physical process of condensation, the prediction of mixed layer thickness was improved, the TKE magnitude decreases, and the time bias of fog formation and dissipation prediction was reduced (Mikio and Hiroshi 2009)
7	Asymmetric Convection Model 2 Scheme (ACM2)	Nonlocal +Local	The upward and downward mixing process were local. First-order Closed Model	The thermal penetration and wind shear of the entrainment layer were considered in the PBL height under unstable conditions. The height of the PBL was determined by the Richardson number (Pleim 2007)
8	Bougeault-Lacarrere Scheme (BouLac)	Local	TKE Closing Scheme, 1.5 Order Closing Model	It could predict the intensity and location of clear-sky turbulence over steep terrain and provide a continuous prediction of turbulent energy intensity (Bougeault and Lacarrere 1989)
9	University of Washington (TKE) Boundary Layer	Local	TKE Closing Scheme, 1.5 Order Closing Model	The introduction of a water vapor conservation variable and explicit entrainment closure was suitable for the case of the dry convective PBL (Bretherton et al. 2009)
10	Shin-Hong Scale-aware	Local	TKE Closing Scheme, 1.5 Order Closing Model	Vertical mixing in a stable PBL and free atmosphere was similar to the YSU scheme, and it could also diagnose TKE and mixed length output (Shin and Hong 2015)
11	Grenier-Bretherton-McCaa	Local	TKE Closing Scheme, 1.5 Order Closing Model	Considered the entrainment process at the top of the PBL, the cloud cover could be well simulated, and the height of the PBL could be calculated according to the grid point heat (Grenier et al. 2001)

Apparently, the PBL wind structures changed substantially under different weather conditions. To clarify the performances of PBL schemes, we evaluated the model results in three weather types, sunny days (24-25 February), haze days (26-27 February) and windy days (28 February-1 March). The model results were interpolated to the DWL position. Then the model and observation data were grouped depending on the observed wind speeds (i.e. <5, 5-10, 10-15 and >15 m s^{-1}) and 6 layer heights (30-100, 100-320, 320-1000, 1000-1500, 1500-2000 and >2000 m) to attain a reliable statistical result. Table 2 lists the paired sample sizes in each group. The statistical quantities for evaluation include the model mean bias, correlation coefficient and standard deviation for the wind speeds and directions between the model results (x) and the observations (y) across N layer heights:

Mean Bias

$$MB = \overline{y} - \overline{x} \quad (1)$$

$$\bar{x} = \frac{1}{N}\sum_{i=1}^{N} x_i \qquad \bar{y} = \frac{1}{N}\sum_{i=1}^{N} y_i \quad (2)$$

Correlation Coefficient

$$CC = \frac{\sum_{I=1}^{N}(y_i-\overline{y})(x_i-\overline{x})}{\sqrt{\sum_{i=1}^{N}(y_i-\overline{y})^2 \sum_{i}^{N}(x_i-\overline{x})^2}} \quad (3)$$

Standard Deviation

$$SD = \sqrt{\frac{1}{N-1}\sum_{i=1}^{N}(x_i - \bar{x})^2} \quad (4)$$

Table 2 The DWL sample size in data groups

	Obs (m. s^{-1})	30-100 m	100-300 m	300-1000 m	1000-1500 m	1500-2000 m	2000-3000 m
Sunny days	0-5	239	342	653	249	87	0
	5-10	1	90	923	719	403	72
	10-15	0	0	56	175	479	748
	> 15	0	0	0	34	131	261
Haze days	0-5	240	420	1056	44	3	0
	5-10	0	0	480	13	96	28
	10-15	0	0	34	270	553	463

	> 15	0	0	0	27	142	424
	0-5	205	257	607	135	86	0
Windy	5-10	34	110	493	314	146	8
days	10-15	1	29	224	221	300	210
	> 15	0	2	308	357	324	271

3. Results

3.1. PBL wind speed profile

Figure 3 shows the PBL wind speed profiles and the model biases with different PBL schemes. The simulated and observed wind speeds varies greatly with altitude. Comparing to Figure 2, most of the PBL schemes captured the evolution of wind speed over the days. During the whole model period, the mean model biases in wind speeds were positive in the layer of 0-1000 m. All PBL schemes had model biases no more than 10 $m.s^{-1}$. The model layers near surface were greatly affected by the roughness length of urban boundary layers which are parameterized in the model with uncertainty. The model biases changed with weather conditions. On haze days (February 26-27), the observed wind speeds were smaller than in the clear days, because the stagnant weather conditions and the aerosol radiative feedback both enhanced the PBL stability and also lowered the surface wind speeds (Sun et al. 2017). For example, when the wind speed was 5-10 $m.s^{-1}$, the simulated wind speed in the haze days was 1-2 $m.s^{-1}$ (18% - 38%) lower than the observed wind speed on each level. On windy days (February 28-March 1), the model bias in wind direction decreased along the height. In the layer of 1000-1500m, the wind direction bias of PBL schemes were 1.1°-9.1° (0.4%-3.4%) (except bias of QNSE was 88°, 33.4%).

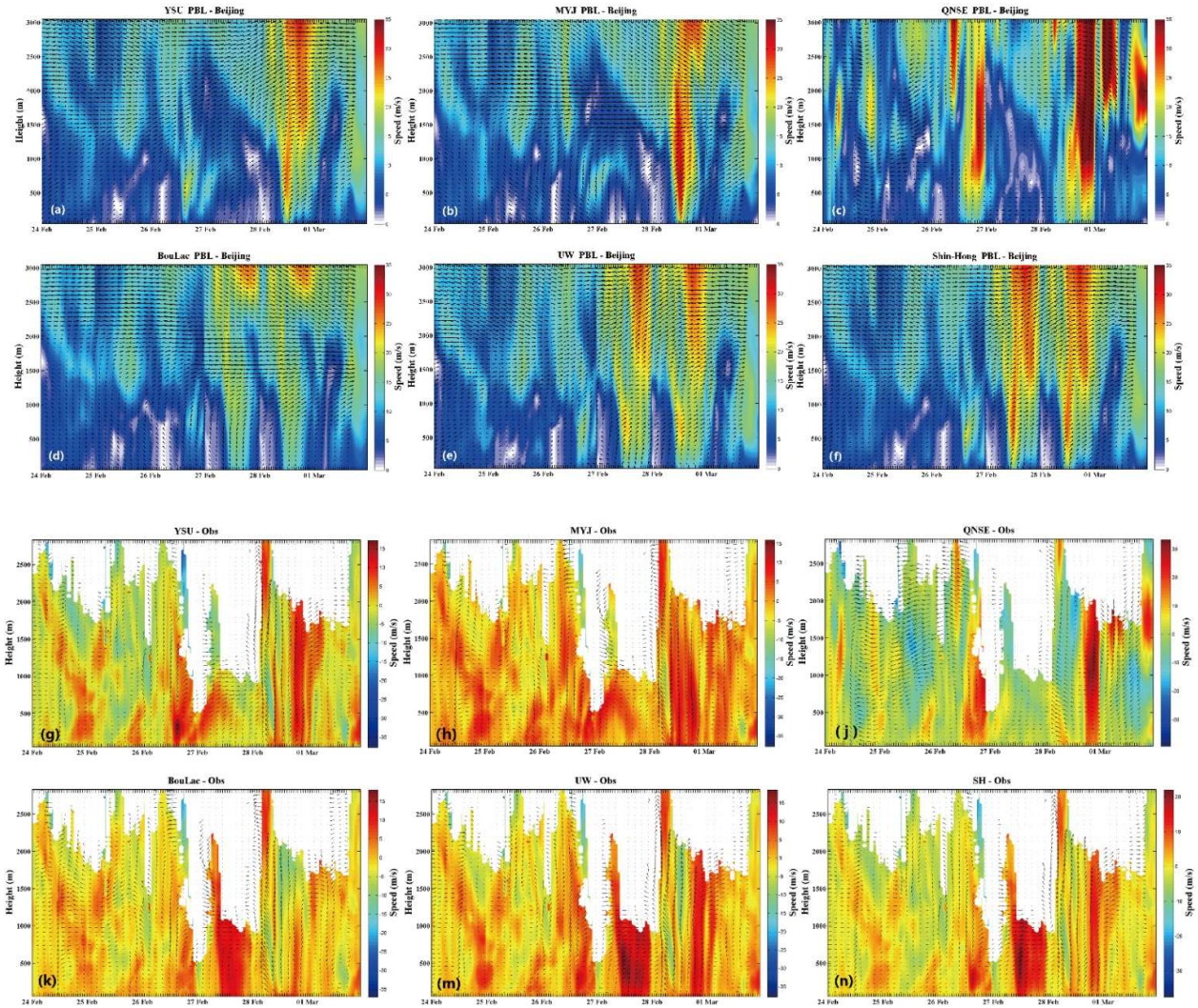

Fig. 3 The wind field simulations (a-f) with the PBL schemes of YSU, MYJ, QNSE, BouLac, UW and Shin-Hong Schemes and their biases (g-n) against the observations. The sunny, haze and windy days were at February 24-25, February 26-27 and February 28 to March 1, respectively.

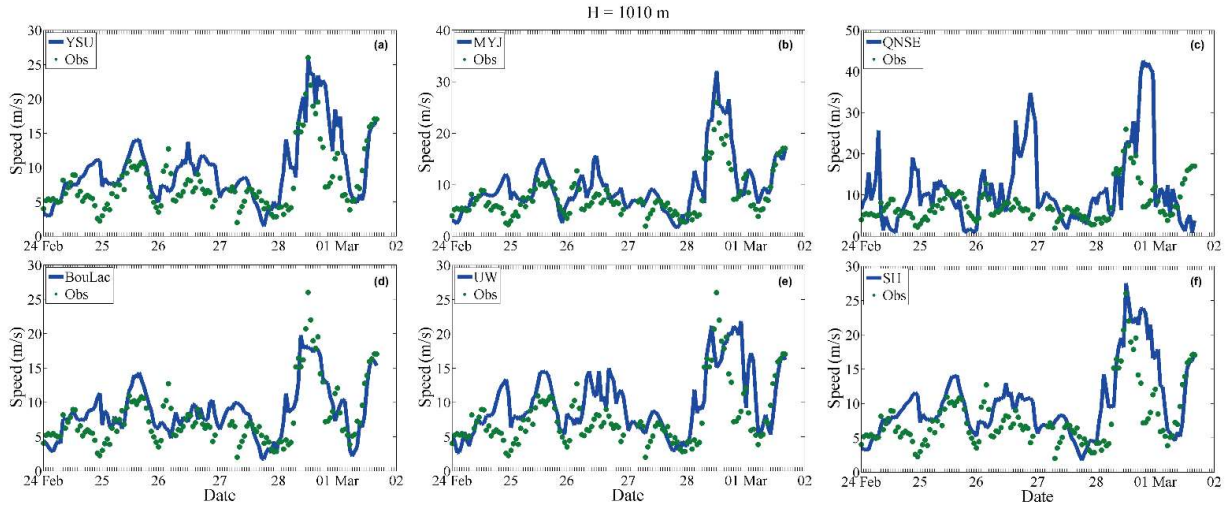

Fig. 4 The observed and simulated wind speeds at 1010 m height with the PBL schemes of YSU, MYJ, QNSE, BouLac, UW and SH.

3.2. Horizontal wind component in PBL

Figure 5 presents the model biases in horizontal wind components at layer in different horizontal speed levels. Generally, all the PBL schemes had the model biases in horizontal wind speed less than 2 m.s^{-1} and the biases in wind direction less than 20°. In gentle windy days with the observed wind speed less than 5 m.s^{-1}, the YSU bias was up to 10 m.s^{-1}. On sunny days and haze days, the model biases of YSU were large at 1000-1500 m and 1500-2000 m where the wind speeds exceeded 15 m.s^{-1}. QNSE showed the maximum model bias in wind speeds, particularly in haze and windy days. On windy days, the biases in wind direction were about 80° or even more than 100° at the heights of 300-1000 m, 1000-1500 m, and 1500-2000 m. Meanwhile, the biases of other PBL schemes were within 20°. The MYJ scheme performed well in the wind speed simulation, but overestimated the wind direction about 280% below 300 m. In the wind speed level of 5-10 m.s^{-1}, the biases in wind direction were over 100° for the schemes of YSU, GFS, MYNN2.5, MYNN3 and BouLac. The model bias also increased with height, particularly when the observed wind speeds were less than 5 m.s^{-1}. On haze days when the wind speed was less than 5 m.s^{-1}, the wind direction biases for these PBL schemes were more than 180° at 1500-2000 m.

Table 3 shows the results with normalized mean biases within 20% of wind direction and speed This table shows the biases of PBL scheme for a specific height and wind speed interval. At 1000-1500 m and 1500-2000 m altitude, the simulated standard deviation was large when the observed wind speeds exceeded 15 m.s^{-1} or less than 5 m.s^{-1}. The QNSE schemes gave a reasonable wind speed and direction value on sunny days, but the model results became worse on haze and windy days. On windy days, the QNSE scheme led to the standard deviations of wind directions at 300-2000 m up to 80° or even more than 100°, while the other schemes had biases within 20°. The MYJ scheme well simulated the wind speed, but the variation of wind direction below 300 m was up to about 280%. The variations of wind directions as using the YSU, GFS, MYNN2.5, MYNN3 and BouLac schemes were over 100° in the wind speed level of 5-10 m.s^{-1}. On haze days, for the wind speed less than 5 m.s^{-1}, the simulated standard deviations of wind direction were more than 180° at 1500-2000 m height.

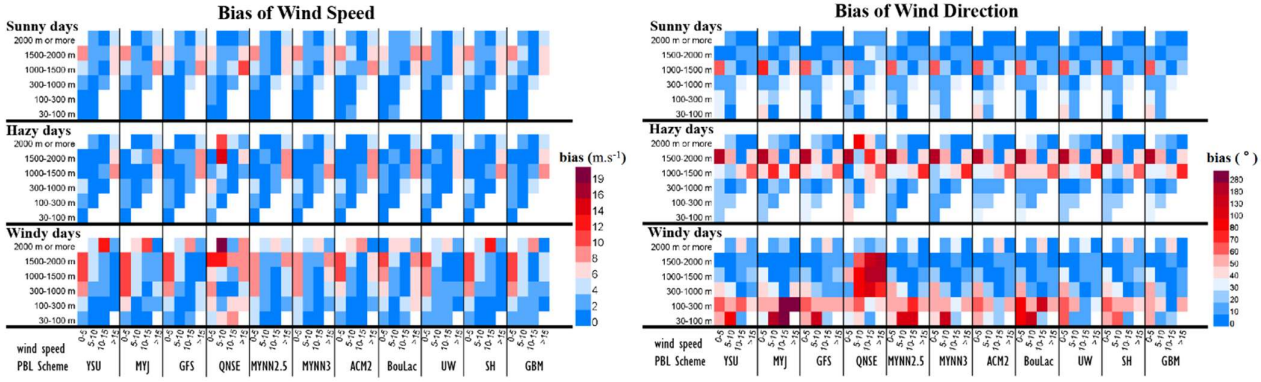

Fig. 5 The model biases in wind speed (left, bias less than 2 m.s^{-1}) and the wind direction (right, bias less than 20°) depending on the PBL schemes, the layer heights and the wind speeds on sunny, haze and windy days.

Table 3 PBL scheme with small bias of wind speed and direction, large correlation coefficient and close standard deviation under three weather conditions and four wind speeds. The bias of suitable scheme is within 20%, and the number is in order.

	Height	Wind speed simulation				Wind direction simulation			
	Obs (m. s^{-1})	0-5	5-10	10-15	>15	0-5	5-10	10-15	>15
Sunny days	30-100 m	③	—	—	—	③⑤⑥	—	—	—
	100-300 m	①②③⑤⑥⑧⑩⑪	②⑤⑪	—	—	⑧	①②③⑤⑥⑧⑨⑩⑪	—	—
	300-1000 m	⑦	③⑦⑨	—	—	①②③⑤⑥⑦⑧⑨⑩⑪	①②③④⑤⑥⑧⑨⑩⑪	—	—
	1000-1500 m	⑧	③⑤⑥	⑦⑧⑨⑩⑪	—	①②③⑤⑥⑦⑧⑨⑩⑪	①②③⑤⑥⑦⑧⑨⑩⑪	①③⑤⑥⑧⑨⑩⑪	—
	1500-2000 m	⑤⑥⑧⑨	①③⑨⑩	⑤⑥⑦⑧	④⑦⑪	⑧	④	②④	②③④⑦⑪
	2000-3000 m	—	—	①②⑤⑥⑦⑧⑨⑩⑪	③④⑤	—	①③⑦⑧⑨⑩⑪	—	②④
Haze days	< 100 m	②③④⑨⑪	—	—	—	A11	—	—	—
	100 - 300 m	②④	⑤⑩	—	—	⑤⑥⑨	④⑥⑨⑪	—	—
	300 -1000 m	③⑧⑪	①②⑦⑨⑩	①②④⑨⑩	—	①②③⑩	①③④⑤⑨⑩⑪⑥⑦	①②③⑤⑥⑦⑧⑨⑩⑪	—
	1000-1500 m	②③	—	②⑦	—	④	—	①③⑤⑥⑦⑧⑨⑩⑪	—
	1500-2000 m	—	①②③⑤⑥⑦⑧⑨⑩⑪	①④⑤⑥⑦⑧⑨⑩⑪	①③④⑤⑦⑧⑨⑩⑪	—	①③④	①②③⑤⑥⑦⑧⑨⑩⑪	②④⑤⑥⑨
	>2000 m	—	①②③⑤⑥⑦⑧⑨⑪	③⑦	①②③⑤⑥⑦⑧⑨⑩⑪	—	①②③⑤⑥⑦⑧⑨⑩⑪	①②③⑤⑥⑦⑧⑨⑩⑪	②③⑨
Windy days	< 100 m	②④	①②④⑤⑥⑦⑨⑩⑪	—	—	②⑧	②④	—	—
	100 - 300 m	①②③④⑧⑩	①③④⑤⑥⑦⑧⑨⑩⑪	—	—	③	②③④⑤⑥⑧⑨	—	—
	300 -1000 m	A11	①⑤⑥⑦⑨⑩⑪	①②③⑤⑥⑦⑧⑨⑩⑪	⑤⑥⑦⑧⑨⑩	④⑪	③⑤⑥⑦⑧⑪	①②③⑤⑥⑦⑧⑨⑩⑪	①③⑤⑥⑦⑧⑨⑩⑪
	1000-1500 m	④⑤⑥⑨	②③⑦⑧⑪	⑨	①⑨⑩⑪	A11	①③⑦⑧⑨⑩⑪	①②③⑤⑥⑦⑧⑨⑩⑪	①②③⑤⑥⑦⑧⑨⑩⑪
	1500-2000 m	⑤	A11	①②③⑤⑥⑦⑧⑨⑩⑪	①②④⑥⑦⑧⑨⑩⑪	①②③⑦⑩⑪	①②④⑤⑥⑦⑧⑨⑩⑪	A11	①②③⑥⑦⑧⑨⑩⑪
	2000-3000 m	—	①②⑦⑧⑨⑩⑪	①②③④⑨⑩⑪	③⑨	—	① ③⑩⑪	A11	②⑧

Table 3 Relative average bias of wind speed and wind direction of 11 PBL schemes in different altitude sections and wind speed sections. Obs represents the range of observed wind speeds, ①②③④⑤⑥⑦⑧⑨⑩⑪ represent the PBL parameterization schemes YSU, MYJ, GFS, QNSE, MYNN2.5, MYNN3, ACM2, BouLac, UW, Shin-Hong, GBM

It is compared in Fig. 6 between the wind field observed near the ground and the simulated wind field with two PBL schemes under the same conditions, when the wind speed was 5-10 m.s^{-1} on sunny days. Figure 7 shows a comparison of different wind speeds and height schemes under three weather conditions. Better simulation of schemes results are presented. We can see from the chart that the wind direction and wind speed simulations can cover the observation results, yet there were still biases, up to 45°- 60°sometimes.

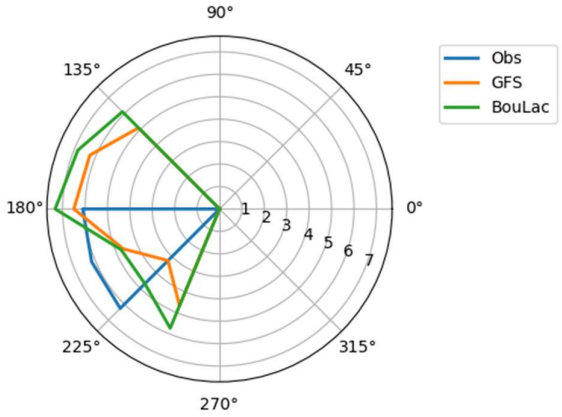

Fig. 6 Wind field comparison chart, the observed wind speed is 5-10 m.s^{-1}, and the height is at 100-300 m on the 24th-25th (sunny days)
Obs stands for observation wind field, GFS scheme simulates the wind field, with wind speed and wind direction bias of 0.68 m.s^{-1} and 9.8 ° respectively, BouLac scheme simulates wind field, with wind speed and wind direction bias of -1.1 m.s^{-1}, 0.8 °.

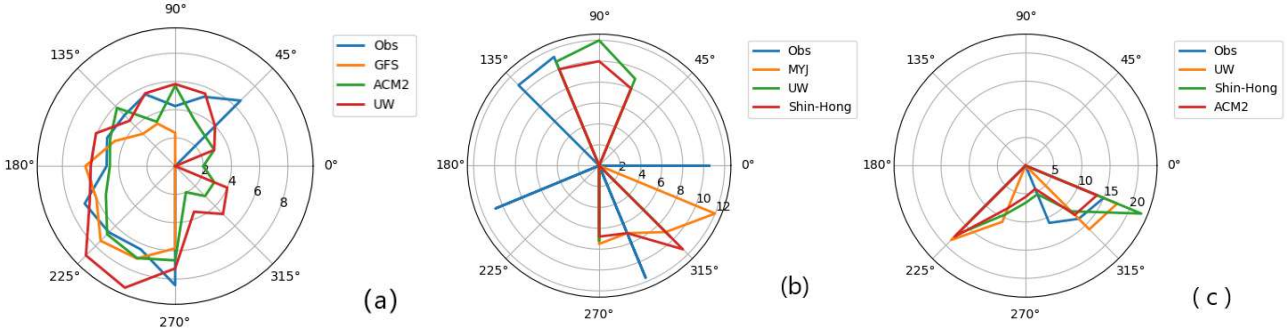

Fig. 7 Wind field comparison chart, the observed wind field and simulated wind field with several PBL schemes under different conditions
(a) On sunny days, at the height of 300-1000 m, 5 < Obs <10 m.s^{-1}, (b) On haze days, at the height of 300-1000 m, 10 < Obs < 15 m.s^{-1}, (c) On windy days, at the height of 1000-1500 m, 10 < Obs < 15 m.s^{-1}

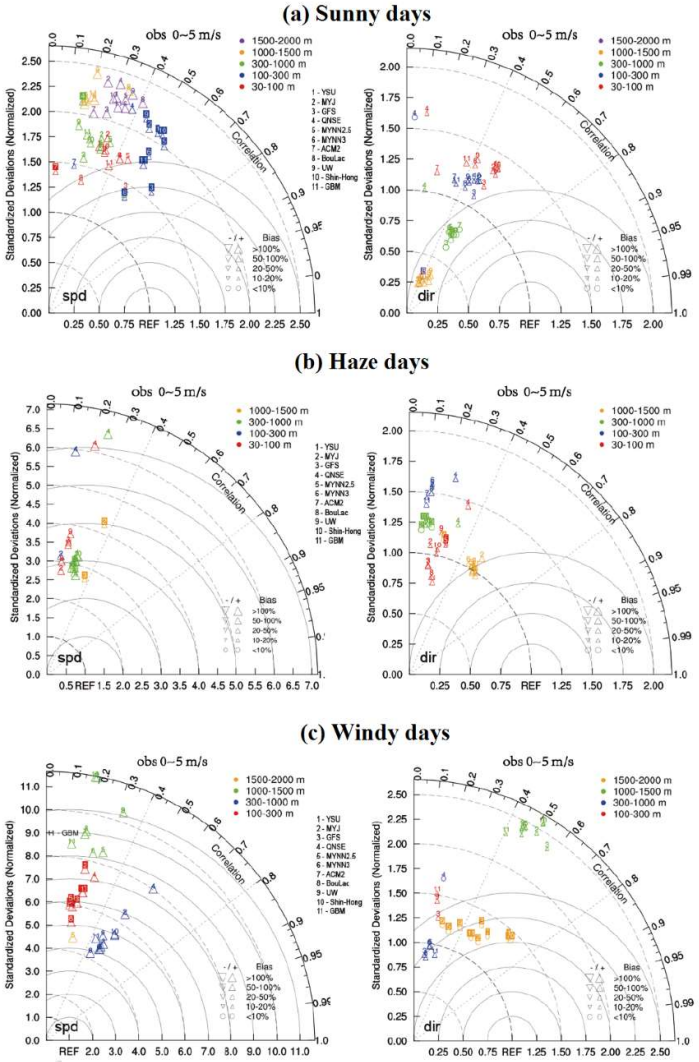

Fig. 8 Taylor charts of mean bias, correlation coefficients and standard deviations for the model results with 11 PBL schemes. On (a) Sunny days (b) Haze days (c) Windy days, with the observed wind speed at 0-5 m.s^{-1}.

Figure 8 exhibits the Taylor chart for the model results at different heights and wind speeds with the observed wind speed is at 0-5 m.s^{-1}. Taylor charts shows the similar characteristics with other observed wind speeds (i.e. 5-10, 10-15 and >15 m.s^{-1}). The correlation coefficients that failed to pass the significance test with the significant level of 0.05 were not shown in the figure. The horizontal and vertical coordinates represent the ratio of the standard deviation of the simulated value to the standard deviation of the observed value. A ratio of 1 indicated that the standard deviation was perfect. The gray arc represents the isoline with equal distance between each point and the point with a standard deviation of 1. In the left and right columns of the figure, 'spd' in the lower left corner stands for the comparison of wind speed between the simulated value and the observed value, and 'dir' represents the comparison of wind direction. Obs represents the actual wind speed range of the analysis data in the graph. The cases with coefficients failed to pass the significance test in three kinds of days did not appear in figures.

As we seen from Figure 8, each wind speed segment could have suitable simulation schemes for each height. Biases and standard deviation should also be considered comprehensively. For example, when the Obs was 5-10 m.s^{-1} the standard deviation at 100-300 m was approximately 20 times higher than the observation standard deviation. The correlation at 300-1000 m was approximately weak as 0.1-0.2, while at 1000-1500 m there was the non-pass hypothesis test. On windy days, when Obs was 0-5 m.s^{-1}, the simulated value of wind speed was several times by the standard deviation of the observed value, and the bias value was more than 100%.

3.3 Classical PBL schemes

As is shown in Section I, many previous studies had indicated that YSU, MYJ, ACM2 had good simulation results. In this study, the PBL conditions changed with the weather evolution and they were not always stable or unstable. On windy days, as the observed wind speed in 5-10 m.s^{-1} and the height greater than 300 m, the YSU bias of wind speed was 50-70%. On sunny days, when the observed wind speed was less than 5 m.s^{-1}, then the MYJ mean bias of wind speed was in 60-290%. A few researches claimed that the QNSE scheme was suitable in stable conditions, which is also proved in our results. We found that the QNSE scheme performed

poorly on windy days but showed better results on sunny days and haze days, especially for the observed wind speed exceeding 5 $m.s^{-1}$ at the layers over 2000 m. The above performances further proves that a scheme cannot be fully suitable for certain weather conditions.

The YSU and MYJ schemes, widely applied in previous studies, also presented good performances in our studies. The YSU scheme may be a good choice under the following conditions: to simulate the surface wind direction for the observed wind speed stronger than 5 $m.s^{-1}$, or to simulate the wind direction above 300 m on sunny and haze days , perhaps to simulate wind speed below 300 m on windy days. It also can be used to simulate the wind direction above 300 m, the wind speed simulation above 1000 m, the wind speed simulation of over 15 $m.s^{-1}$ and the wind direction simulation of 5-15 $m.s^{-1}$.

The MYJ scheme was considered suitable for the following conditions. For example, to simulate wind speed below 300 m when the wind speed is more than 5 $m.s^{-1}$ on sunny days, or to simulate the winds at 300-1000 m, perhaps to simulate the wind direction when the height is greater than 1000 m, maybe also on windy days when the wind speed is in 10-15 $m.s^{-1}$ and the altitude is greater than 2000 m. Besides, the MYJ scheme is able to well capture both wind speed and direction on haze days when the wind speed was 10-15 $m.s^{-1}$ at 300-1000 m.

In other words, the suitable PBL schemes should be chosen under different conditions. In this case, on sunny days, when Obs was 0-5 $m.s^{-1}$, we found that the wind speed simulated well at the height 100-300 m, and the wind direction simulation performed well at 300-1000 m. When the Obs was 5-10 $m.s^{-1}$, the wind speed at 100-300 m was better than at 300-1000 m. When the Obs was 10-15 $m.s^{-1}$, the wind speed data mainly distributed in the upper 1000 m, while little data at 1000-2000 m satisfied hypothesis test, and much data satisfied hypothesis test at the height above 2000 m. At this altitude, we can use the scheme 7 and 12. The wind speed greater than 15 $m.s^{-1}$ was mainly distributed at the height above 1500 m, and scheme 2, 4, 7 and 11 could be selected. On haze days, when the height was above 1000 m, the simulation results of several schemes were better. When the Obs was less than 5 $m.s^{-1}$ and the height was 1000-1500 m, the wind direction could be simulated with the PBL scheme 2 and 3, and the wind speed simulation at 300-1000 m was relatively well. Above 2000 m, the simulation results cannot be verified completely due to limited observation data. It turns out that no PBL scheme could always show good performances.

3.4 Vertical wind component in PBL

Figure 9 shows the observation and the simulated vertical wind speeds with three PBL schemes. According to the observed vertical wind field. On sunny days and haze days, the simulated wind speed values were 10% of the observation value, and the wind speed is mostly distributed between 0-0.5 under the boundary layer, and the wind direction is vertical downward. However, the simulation results show that the wind direction is mainly vertical upward. On the windy days from Feb. 28 to March 1, there were strong upward turbulence from surface to the upper air in the vertical direction, and the maximum wind speed is more than 0.5$m.s^{-1}$.

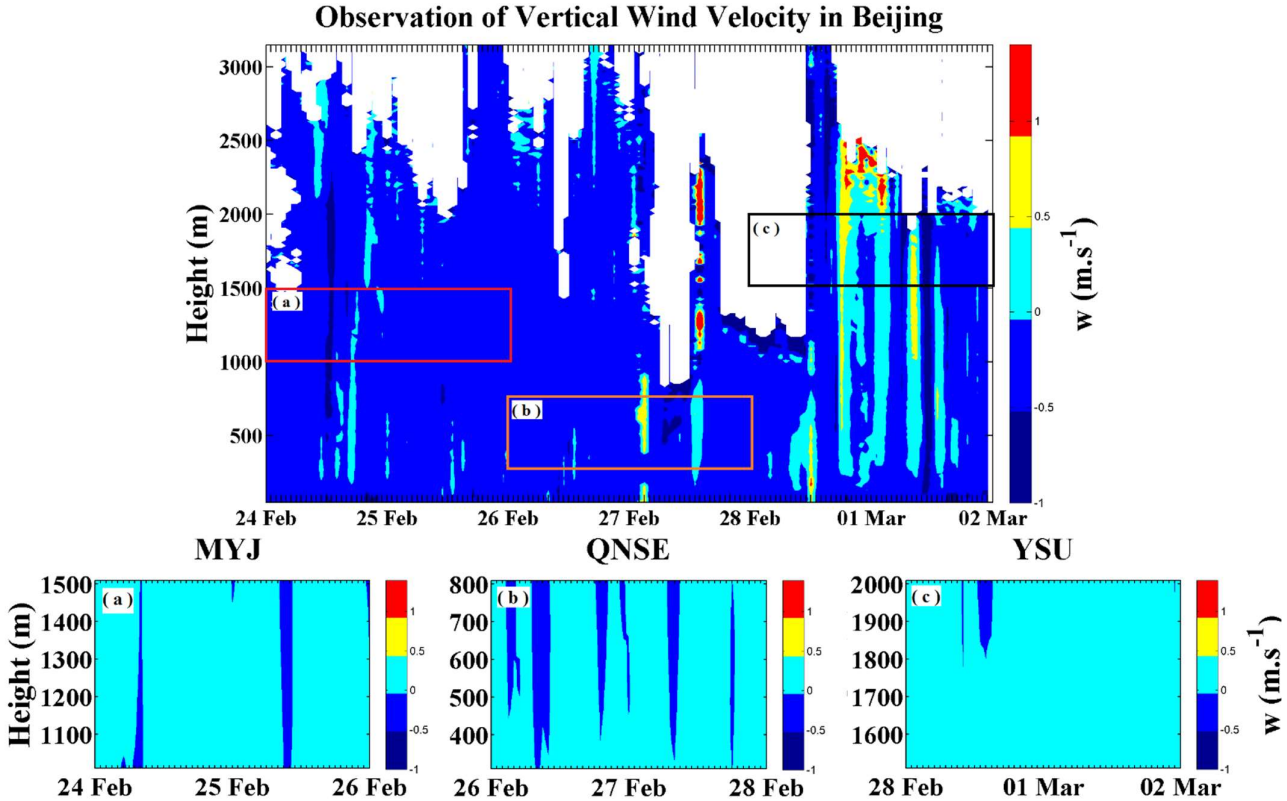

Fig. 9 Comparison of vertical wind speeds between the observations and the simulations using (a) the GFS scheme at 1000-1500 m height on sunny days, (b) the MYNN3 scheme at 300-800 m height on haze days, and (c) the UW scheme at 1500-2000 m height on windy days.

The model failed to capture the change in vertical wind speeds. Not only as a consequence of the model's uncertainty, but also could be the biases in the DWL data. It is known that, under clear sky, the updraft and downdraft of airflow were small. The turbulence echo approached the detection limit of the Doppler lidar, which makes an accurate extraction of vertical wind speed difficult.

4. Conclusions

In this study, the accuracy of vertical wind field simulation for different boundary layer schemes are systematically evaluated by high-resolution wind Doppler lidar for the first time, with a typical process simulated by WRF model in Beijing. The results show that the wind field simulated well at a height of 1000-2000m, as most of the relative mean bias of wind speed and wind direction are less than 20% and 6% respectively. Below 1000 m, the wind speed and direction biases are about 30% to more than 150% $m.s^{-1}$ and 6%-30% respectively. The relative mean bias of simulated wind profile is up to 50-300% when the wind speed is lower than 5 $m.s^{-1}$ in the boundary layer. As the wind speed range is 10-15$m.s^{-1}$, the model results are better than other speeds, and is better when the height above 1000m. The PBL schemes have different capabilities to reproduce the changes of wind speed profiles under different weather conditions. An appropriate PBL scheme is dependent on the weather conditions, and the model biases showed substantial changes at height and in different wind speed ranges, and some PBL schemes were not always likely to be suitable for a certain weather condition. The influence of observation height to the assessment was larger than that due to employing the different PBL schemes. This study provides a reference for further improving the development and utilization of wind energy and the accuracy of complex wind field prediction.

Acknowledgements This study was partially supported by the CAS Strategic Priority Research Program (XDA23020301), the National Key Research and Development Program of China (2016YFC0202001) and the National Natural Science Foundation of China (42061130215).

Reference list

Fekih A, Mohamed A (2019) Evaluation of the WRF model on simulating the vertical structure and diurnal cycle of the atmospheric boundary layer over Bordj Badji Mokhtar (southwestern Algeria). Journal of King Saud University-Science 31(4):602-611. https://doi.org/10.1016/j.jksus.2017.12.004

A SG, G SG, A KZ et al (2020) Sensitivity of WRF-simulated 10m wind over the Persian Gulf to different boundary conditions and PBL parameterization schemes. Atmospheric Research 247. https://doi.org/10.1016/j.atmosres.2020.105147

Banks RF, Tiana-Alsina J, Rocadenbosch F et al (2015) Performance Evaluation of the Boundary-Layer Height from Lidar and the Weather Research and Forecasting Model at an Urban Coastal Site in the North-East Iberian Peninsula. Boundary-Layer Meteorol 157:265–292. https://doi.org/10.1007/s10546-015-0056-2

Banks RF, Baldasano JM (2016) Impact of WRF model PBL schemes on air quality simulations over Catalonia, Spain. Science of the total environment 572:98-113. https://doi.org/10.1016/j.scitotenv.2016.07.167

Bougeault P, Lacarrere P (1989) Parameterization of Orography-Induced Turbulence in a Mesobeta-Scale Model. Monthly Weather Review 117(8):1872-1890. https://doi.org/10.1175/1520-0493(1989)117<1872:POOITI>2.0.CO;2

Bretherton CS, Park S (2009) A New Moist Turbulence Parameterization in the Community Atmosphere Model. Journal of Climate 22(12):3422-3448. https://doi.org/10.1175/2008JCLI2556.1

Brewster KA (1989) Profiler Training Manual #2: Quality Control of Wind Profiler Data. NOAA/ERL/FSL, Boulder, CO, and NOAA/NWS/OM, Silver Spring, MD., pp109.

Cheng FY, Chin SC, Liu TH (2012) The role of boundary layer schemes in meteorological and air quality simulations of the Taiwan area. Atmospheric Environment 54(4):714–727. https://doi.org/10.1016/j.atmosenv.2012.01.029

Clark AJ, Gallus WA, Chen TC (2007) Comparison of the Diurnal Precipitation Cycle in Convection-Resolving and Non-Convection-Resolving Mesoscale Models. Monthly Weather Review, 135(10):3456-3473.https://doi.org/0.1175/MWR3467.1

Coantic M, Seguin B (1971) On the interaction of turbulent and radiative transfers in the surface layer. Boundary-Layer Meteorology 1(3):245-263. https://doi.org/10.1007/BF02186030

Muñoz-Esparza D, Cañadillas B, Neumann T, Beeck JV (2012) Turbulent fluxes, stability and shear in the offshore environment: mesoscale modelling and field observations at FINO1. Journal of Renewable & Sustainable Energy 4(6):245-240. https://doi.org/10.1063/1.4769201

Grenier H, Bretherton CS (2001) A Moist PBL Parameterization for Large-Scale Models and Its Application to Subtropical Cloud-Topped Marine Boundary Layers. Mon. Wea. Rev 129(3):357. https://doi.org/10.1175/1520-0493(2001)129<0357:AMPPFL>2.0.CO;2

Hahmann AN, Draxl C, Peña A, Nielsen JR (2011) Simulating the Vertical Structure of the Wind with the Weather Research and Forecasting (WRF) Model. European Wind Energy Conference and Exhibition 153.

Han Z, Zhang M, An J (2009) Sensitivity of air quality model prediction to parameterization of vertical eddy diffusivity. Environmental Fluid Mechanics 9(1):73-89. https://doi.org/10.1007/s10652-008-9088-1

Janjic ZI (1994) The Step-Mountain Eta Coordinate Model: Further Developments of the Convection, Viscous Sublayer, and Turbulence Closure Schemes. Monthly Weather Review 122(5):927. https://doi.org/10.1175/1520-0493(1994)1222.0.CO;2

Huang M, Gao Z, Miao S, Chen F (2019) Sensitivity of urban boundary layer simulation to urban canopy models and pbl schemes in beijing. Meteorol Atmos Phys 131:1235–1248. https://doi.org/10.1007/s00703-018-0634-1

Hong SY, Noh Y, Dudhia J (2005) A New Vertical Diffusion Package with an Explicit Treatment of Entrainment Processes. Monthly Weather Review 134(9):2318-2341. https://doi.org/10.1175/MWR3199.1

Hong SY, Pan HL(1996) Nonlocal Boundary Layer Vertical Diffusion in a Medium-Range Forecast Model. Monthly Weather Review 124(10):2322-2339. https://doi.org/10.1175/1520-0493(1996)1242.0.CO;2

Miglietta MM, Zecchetto S, Biasio FD (2010) WRF model and ASAR-retrieved 10 m wind field comparison in a case study over Eastern Mediterranean Sea. Advances in ence and Research 4:83-88. https://doi.org/10.5194/asr-4-83-2010

Mikio N, Hiroshi N (2006) An Improved Mellor–Yamada Level-3 Model: Its Numerical Stability and Application to a Regional Prediction of Advection Fog. Boundary-Layer Meteorol 119:397–407. https://doi.org/10.1007/s10546-005-9030-8

Mikio N, Hiroshi N (2009) Development of an Improved Turbulence Closure Model for the Atmospheric Boundary Layer. Journal of the Meteorological Society of Japan 87(5):895-912. https://doi.org/10.2151/jmsj.87.895

Pleim JE (2007) A Combined Local and Nonlocal Closure Model for the Atmospheric Boundary Layer. Part I: Model Description and Testing. Journal of Applied Meteorology & Climatology 46(9):1383-1395. https://doi.org/10.1175/JAM2539.1

Sun K, Liu H, Wang X et al (2017) The Aerosol Radiative Effect on a Severe Haze Episode in the Yangtze River Delta. J Meteorol Res 31:59-67. https://doi.org/10.1007/s13351-017-7007-4

Sun Y, Song T, Tang G et al (2013) The vertical distribution of PM2.5 and boundary-layer structure during summer haze in Beijing. Atmospheric Environment 74(aug.): 413-421. https://doi.org/10.1016/j.atmosenv.2013.03.011

Shimada S, Ohsawa T, Chikaoka S et al (2011) Accuracy of the wind speed profile in the lower PBL as simulated by the WRF model. Sola 7: 109-112. https://doi.org/10.2151/sola.2011-028

Sukoriansky S, Galperin B, Perov V (2005) Application of a New Spectral Theory of Stably Stratified Turbulence to the Atmospheric Boundary Layer over Sea Ice. Boundary-Layer Meteorol 117:231–257. https://doi.org/10.1007/s10546-004-6848-4

Shin HH, Hong S (2015) Representation of the Subgrid-Scale Turbulent Transport in Convective Boundary Layers at Gray-Zone Resolutions. Mon. Wea. Rev. 143:250–271, https://doi.org/10.1175/MWR-D-14-00116.1

Wei J, Tang G, Zhu X et al (2017) Thermal internal boundary layer and its effects on air pollutants during summer in a coastal city in North China. Journal of Environmental Sciences 70:37-44. https://doi.org/10.1016/j.jes.2017.11.006

Wang L, Zhang N, Liu Z et al (2015). The influence of climate factors, meteorological conditions, and boundary-layer structure on severe haze pollution in the beijing-tianjin-hebei region during january 2013. Advances in Meteorology, 2014:1-14. https://doi.org/10.1155/2014/685971

Wang Z, Cao X, Zhang L et al (2012) Lidar measurement of planetary boundary layer height and comparison with microwave profiling radiometer observation. Atmospheric Measurement Techniques 5:1965-1972. https://doi.org/10.5194/amtd-5-1233-2012

Wang W, Shen X, Huang W (2016) A Comparison of Boundary-Layer Characteristics Simulated Using Different Parametrization Schemes. Boundary-Layer Meteorol 161:375–403. https://doi.org/10.1007/s10546-016-0175-4.

Zhan L, Shu J, Chen L (2017) Distribution characteristics of wind and pollutant concentration fields in a parallel urban block. Journal of Meteorology and Environment 33(5):61-67.

Zhang C, Wang D, Gong Y (2015) Dynamic Modeling Study of Highly Resolved Near-Surface Wind Based on WRF/CALMET. Meteorological Monthly, 1:34-44.